Upper ocean variability in the Bay of Bengal during the tropical cyclones Nargis and Laila

K. Maneesha,[1*] V. S. N. Murty,[1] M. Ravichandran,[2] T. Lee,[3] Weidong Yu,[4] and M. J. McPhaden[5]

[1] Council of Scientific and Industrial Research (CSIR), National Institute of Oceanography Regional Center Visakhapatnam – 530 017, India

[2] Indian National Centre for Ocean Information Services, Hyderabad, India

[3] Jet Propulsion Laboratory, California Institute of Technology, Pasadena, California, USA

[4] Lab. Ocean-Atmosphere Interaction and Climate Change, First Institution of Oceanography, SOA, Qingdao, China

[5] NOAA/Pacific Marine Environmental Laboratory, Seattle, Washington, USA

* Corresponding author: kkpalli_manisha@yahoo.com

Address:
       K.Maneesha
       CSIR Senior Research Fellow
       National Institute of Oceanography Regional Centre
       176, Lawsons Bay Colony
       Visakhapatnam – 530 017
       India
       Tel. No. +91-(0)891-2784570 (office)
       Fax No. +91-(0)891-2543595
       E-mail: kkpalli_manisha@yahoo.com

Abstract :

[1] Upper ocean variability at different stages in the evolution of the tropical cyclones Nargis and Laila is evaluated over the Bay of Bengal (BoB) during May 2008 and May 2010 respectively. Nargis initially developed on 24 April 2008; intensified twice on 27-28 April and 1 May, and eventually made landfall at Myanmar on 2 May 2008. Laila developed over the western BoB in May 2010 and moved westward towards the east coast of India. Data from the Argo program, the Research Moored Array for African-Asian-Australian Monsoon Analysis and prediction (RAMA), and various satellite products are analyzed to evaluate upper ocean variability due to Nargis and Laila. The analysis reveals pre-conditioning of the central BoB prior to Nargis with warm (>30°C) Sea Surface Temperature (SST), low (<33 psu) Sea Surface Salinity (SSS) and shallow (<30 m) mixed layer depths during March-April 2008. Enhanced ocean response to the right of the storm track due to Nargis includes a large SST drop by ~1.76°C, SSS increase up to 0.74 psu, mixed layer deepening of 32 m, shoaling of the 26°C isotherm by 36 m and high net heat loss at sea surface. During Nargis, strong inertial currents (up to 0.9 ms^{-1}) were generated to the right of storm track as measured at the RAMA buoy, producing strong turbulent mixing that lead to the deepening of mixed layer. This mixing facilitated entrainment of cold waters from as deep as about 75 m and, together with net heat loss at sea surface and cyclone-induced subsurface upwelling, contributed to the observed SST cooling in the wake of the storm. A similar upper ocean response occurs during Laila, though it was a significantly weaker storm than Nargis.

Key words: Bay of Bengal, tropical cyclones, Nargis, Laila, mixed layer, salinity stratification, sea surface salinity, latent heat flux

1. Introduction

[2] The Bay of Bengal experiences intense tropical cyclones during April – May and October – November, with a considerable interannual variability both in the number and intensity of cyclones [*Anonymous,* 1979; *Obasi,* 1997]. Many studies reported that cyclones are responsible for the decrease in SST by 0.3°C to 3.0°C over the BoB depending on the strength and path of the cyclones [*Rao*, 1987; *Gopalakrishna et al.*, 1993; *Chinthalu et al.*, 2001; *Subrahmanyam et al.*, 2005; *Sengupta et al.*, 2007]. Moreover, abnormal cooling of 6°C was reported in the satellite measured SST during Super cyclone Orissa in 1999 [*Sadhuram*, 2004]. In the southern and western parts of the BoB, where salinity stratification is weak in May, larger SST cooling up to 2-3°C and deepening of mixed layer up to 80 m due to cyclones were reported [*Rao*, 1987; *Gopalakrishna et al.*, 1993]. However, in the northern Bay, where salinity stratification is intense, the SST cooling due to monsoon depressions was only up to 0.3°C, as entrainment of cold waters did not reach up to sea surface [*Murty et al.*, 1996; *Sengupta et al.*, 2007]. In all these studies, subsurface variability under the influence of cyclones was not examined due to lack of *in situ* observations. In the present study an attempt is made to study surface and subsurface variability under the influence of cyclones Nargis and Laila using available in situ as well as satellite data products. Some silent features of these cyclones are extracted from the weekly weather reports of the India Meteorological Department (IMD, 2008, 2010) and provided below for ready reference:

[3] Cyclone Nargis sustained over the BoB during 24 April – 3 May 2008. Initially, it formed as a low pressure system and developed into a depression over the southeastern BoB at 0300 UTC of 27April, 2008 with a central pressure of 998 hPa and the associated winds of with 13 ms^{-1}. Under favorable conditions like warmer SST, low to moderate vertical wind shear and upper level divergence, it intensified into a named cyclonic storm (Nargis) at 0300 UTC of 28 April and into a very severe cyclonic storm with a central pressure of 980 hPa at 0300 UTC of 29 April (Fig.1d lower box). The system continued to intensify even after the recurvature over the central Bay with a fall in central pressure up to 962 hPa associated with strong winds up to 46 ms^{-1} (Fig.1d upper box). The system moved almost in easterly direction from 0600 UTC of 1 May and crossed southwest coast of Myanmar near Latitude 16° N between 1200 and 1400 UTC of 2 May, 2008.

Nargis made land fall at Myanmar on 2 May 2008 with winds equivalent to a category 3-4 hurricane [*McPhaden et al.*, 2009a]. The system maintained the intensity of cyclonic storm for about 12 hrs after the landfall causing extensive loss of life and property (IMD, 2008). It was the worst natural disaster to affect the Indian Ocean region since the Asian tsunami in December 2004. This cyclone

left in its wake a swath of destruction along with over 130,000 dead and missing and billions of dollars of economic loss.

Cyclone Laila developed over the BoB during 17-22 May 2010. A low pressure area developed in the southeastern BoB on 17May 2010 with a central pressure of 998 hPa associated with 15 ms^{-1} winds. It moved in a northwesterly direction and intensified into a severe cyclonic storm Laila. Moving in a west-northwesterly direction, it crossed the Andhra Pradesh coast near Bapatla, about 50 km southwest of Machilipatnam, between 1100 and 1200 UTC of 20 May 2010 as a severe cyclonic storm with a central pressure of 986 hPa. It then recurved north-northeastwards and weakened gradually. The cyclone slowed down after making landfall and maintained cyclone intensity for about 12 hrs afterwards. It was the first severe cyclone to cross the Andhra Pradesh coast since 1990 in the month of May (IMD, 2010).

[4] The international oceanographic community has been involved over the past several years in developing an integrated observing system in the Indian Ocean for climate research and forecasting. Elements of this Indian Ocean Observing System (IndOOS) captured the development of cyclone Nargis as it grew in strength and migrated eastward across the BoB in late April 2008. *McPhaden et al.* [2009a] described preliminary aspects of the air-sea interaction associated with the Nargis. In the present paper, focus is given to the 3-D structure of upper ocean variability using *in situ* temperature and salinity data from the Argo floats in the vicinity of Nargis's and Laila's tracks. Surface meteorological and upper ocean data from RAMA buoys along 90°E between Equator and 15°N [McPhaden *et al.*, 2009b] and satellite data products of surface wind speed and wind stress curl derived from the QuikSCAT scatterometer are also analyzed to document the variability in the oceanic response due to these cyclones.

2. Data

[5] In this study, we utilize the *in situ* observations obtained from Argo profiles (INCOIS 2010) and from RAMA buoys during the passage of intense tropical cyclones Nargis and Laila. Cyclone track data at every 3 hours, including centre location, centre pressure and maximum sustained wind speeds are obtained from QuikSCAT derived surface winds and wind stress curl data are also utilized. The Argo temperature and salinity profiles are obtained at 5 day repeat cycles and 10 day repeat cycles. However we used the 10 day repeat cycles data from all the floats in the entire study. Values of temperature and salinity at 4 m depth in Argo profiles are considered as SST and SSS respectively. For RAMA buoys data, water temperature closest to the surface at 1 m depth is considered as the

SST. Since strong salinity stratification prevails and barrier layers exists in the upper ocean of the BoB [Murty *et al.*, 1996, Vinayachandran *et al.*, 2002, Pankajakshan *et al.*, 2007], the MLD is estimated from the density profiles as the depth at which water density is higher by 0.2 Kgm^{-3} than the surface density [McPhaden *et al.*, 2009a] using Argo and RAMA data. The upper layer heat content (HC) in 0-30 m, 0-50 m and 0-100 m layers and the cyclone heat potential (CHP), relative to 26°C isotherm (D26) are computed following procedures outlined by Murty *et al.* [1996] and Sadhuram *et al.* [2004]. The rates of change of CHP and HC over 10 day periods in different layers are also estimated.

3. Results and discussion

[6] 3.1 *Variability in the cyclone tracks of Nargis and Laila*

The climatology of the cyclone tracks in the month of May shows that most of the cyclones moved westward and northward during 1945-1970 (Fig. 1a), while in recent decades (1970-2008) the cyclones moved northward/northeastward (Fig. 1b). Nargis formed over the BoB on 24 April 2008 and initially moved northwestward and intensified during 27– 28 April. It was predicted to hit the Indian coast, but it abruptly turned northeastward and intensified into a cyclone on 1 May 2008 (Red track in Fig. 1b and Fig. 1c). Laila moved in the northwesterly direction and intensified on 18th of May 2010 after passing over warm surface waters. On 20th May, it moved slowly and intensified further to a severe cyclonic storm and made landfall near Bapatla, Andhra Pradesh (Blue track in Fig. 1b and Fig.1d).

[7] *3.2 Estimated changes in the oceanic parameters and currents due to Nargis*

Eight Argo profiles are available in the vicinity of the cyclone track for Nargis, (Fig. 1c). Figs. 2a-f show the estimated change (after minus before the passage of cyclone Nargis) in SST, SSS, D26, MLD, CHP and HC in the 0-30 m layer (HC30). These anomalies show the large-scale impact of Nargis on the upper ocean. Floats #768, #673, #672, #755 and #675 are the nearest on either side of cyclone track over which the Nargis intensified (marked in boxes on the track in Fig. 1c). The impact is larger on the right of cyclone track with a drop in SST between -1.2°C and -1.8°C (Fig. 2a), increase in SSS between 0.20 and 0.74 psu (Fig. 2b), shoaling of D26 between -9 and -22 m (Fig. 2c) and deepening of mixed layer between 22 and 32 m (Fig. 2d). Moreover, it is observed that in regions farther from the cyclone's influence, the MLD is unaffected, but the D26 deepened (Figs. 2c-d). The estimated rate of change in CHP was negative and varied between -139 and -394 Wm^{-2}, suggesting larger heat loss in response to Nargis (Fig. 2e). It appears that most of the CHP loss

occurred in the upper 30 m layer with the change in HC30 occurred between -109 and -182 Wm^{-2} (Fig. 2f).

Cyclone Nargis intensified to super cyclone strength on 1 May 2008 (marked with a second rectangular box on the track in Fig. 1c). At this time, it passed closer to the float #755, which was about 20 Km to the right of the track. At this location, the SST drop was -1.2°C (Fig. 2a) and heat loss was also high as evident from the rates of change in CHP and HC30 (Figs. 2e-f).

[8] Another noteworthy observation is that at float #673, which is about 100 Km to the right of the storm track, SST decreased by 2°C, SSS increased by 0.74 psu, MLD deepened by more than 30 m and the upper ocean heat loss was also significant in the top 30 m on the right side of cyclone track. In general, the strongest winds are found on the right side of the cyclone track mainly due to the fact that the forward motion of the cyclone also contributes to its cyclonically rotating winds (Novlan *et al.*, 1974, McPhaden *et al.*, 2009a), so the turbulence generated by these strong winds would increase vertical mixing. Chinthalu *et al.* (2001) reported the measurements of inertial oscillations at 2.5 m depth from a surface buoy in the central BoB due to the passage of a tropical cyclone (No name was given to this), with the magnitude of inertial currents reaching 0.80-0.90 ms^{-1}. Using data from surface drifter buoys drogued at 15 m depth in the central BoB, Saji *et al.* (2000) also reported the occurrence of inertial currents with clockwise rotation in the wake of a storm. Figs. 3a-b show the RAMA buoy (15°N, 90°E) measured currents at 10 m depth during 1 April – 31 May, 2008 covering the Nargis period, and the generation of inertial oscillations of 2 day period due to Nargis. Prior to Nargis, the time variation of daily averaged zonal and meridional currents show predominantly northwestward flow with a biweekly (14 day) oscillation in zonal currents and shorter period (5-10 day) oscillations in meridional currents (Fig. 3a). During the passage of Nargis (shown by dashed vertical lines), northeastward flow is dominant with strong (0.30 ms^{-1}) eastward and northward components. Because of the strong cyclonic winds, inertial oscillations were generated with a period of 2 days, which is close to the local inertial period (~46.4 hours) at 15°N latitude. The existence of inertial currents is more evident in the high resolution 2-hourly current vectors shown in Fig. 3b for the period 29 April – 5 May. After Nargis passed, the biweekly oscillations in the zonal flow were replaced by shorter period oscillations (<10 day period), while the meridional flow was predominantly southward. The generation of inertial oscillations due to cyclonic wind forcing and the associated turbulent mixing on the right of the cyclone track would also facilitate mixed layer deepening and cooling (Price, 1981) as observed in Fig. 2. Behra *et al.* (1998) investigated the BoB response to the cyclones in a simple ocean model. In this model with a translating cyclone embedded

in symmetric background wind forcing, both the circulation and upper layer thickness deviation are found to be asymmetric relative to the storm center, with maximum magnitude of flow located to right of the storm track. These authors attributed this right bias to the presence of inertial currents. Wind stress rotates in the same direction as upper ocean inertial currents on the right side of the track and opposite on the left of the track. The vertical shear associated with these inertial currents in the mixed layer contributed to the deepening of mixed layer and cooling of the surface.

[9] *3.3 Temporal variations in the oceanic parameters and net surface heat flux*

We examined further the temporal variations of SST, SSS, wind speed, net surface heat flux, MLD, D26, HC30 and CHP using daily averaged RAMA data at 15°N, 90°E and the same parameters (except wind speed and net heat surface flux) using Argo data close to the RAMA buoy during 1 March – 9 June, 2008 covering the Nargis period (Figs. 4a-h). Significant temporal variations are seen in all parameters, especially SST, SSS, MLD, D26 and CHP. RAMA data show a decrease in SST, reduction in upper ocean heat content and an increase in SSS and MLD in response to Nargis (Figs. 4a, 4b). From March 2008 onwards, SST showed warming trend up to 30.5°C on 21 April and then sharply decreased to 28.0°C during Nargis (Fig. 4a). The RAMA buoy recorded the lowest SSS (<31.5 psu) in early April 2008 (Fig. 4b) and then slightly increased during Nargis due to turbulent mixing in the upper mixed layer and entrainment of subsurface high salinity waters into the mixed layer (McPhaden *et al.*, 2009a). Higher surface winds (Fig. 4c) due to Nargis enhanced the latent heat flux and contributed to a large drop in net surface heat flux (Fig. 4d), as provided by the PMEL/NOAA. The observed higher SSS in Argo data compared to RAMA data affected the MLD estimations (Fig. 4e), but during Nargis, both the MLD estimates showed similar increase and deepening of mixed layer. Like SST, HC30 also showed a build up from January till the development of Nargis, but decreased abruptly by 30 Wm^{-2} due to Nargis's passage; the large decrease is particularly pronounced in the RAMA data (Fig. 4f). The Argo data showed an increasing trend in both D26 and CHP from March to the Nargis period and then suddenly dropped by 24 m and 30 Wm^{-2} (Figs. 4g-h) respectively due to Nargis. Variations in the high resolution RAMA data derived D26 and CHP (Figs. 4g-h) highlight the importance of dynamics below the mixed layer (Fig. 4e). While SST decreased from 24 April to 1 May (covering the first and second intensification phases of Nargis), the rates of change in HC30 and CHP indicated that the first intensification (27-28 April) occurred when the upper ocean possessed higher HC30 and CHP. This feature is missing from Argo data due to lower resolution (5-10 day interval). However, the upper ocean heat loss (indicated by

decreasing values of HC30 and CHP) during the second intensification of Nargis is well represented by both RAMA and Argo data sets (Figs. 4f &h).

[10] *3.4 Depth-time sections of temperature and salinity from Argo data during Nargis*

Argo data are used to construct depth-time sections of temperature (Fig. 5) and salinity (Fig. 6) along two transects (shown as A-A1 and B-B1in Fig. 1c) to examine the 3-D structure of upper ocean variability and stratification across and along Nargis track. Prior to Nargis, a pocket of very cold water with temperature <26.5°C (Fig. 5) and low salinity of <33.0 psu (Fig. 6) representing winter conditions extended up to 40 m during January 2008 on the north/northeastern part of the cyclone track. In January, MLD varied between 10 m in the north and 60 m in the central Bay, which is evident in both sections. One week prior to Nargis along the A-A1 section, the seasonal spread of low salinity water (<33 psu) to greater depths followed by vertical mixing (isohalines occupy greater depths) towards the central Bay is evident; spring warming occurred over a 60 m thick layer with a rise in temperature to about 2.5°C by April in the central Bay and the associated MLD is shallow varying between 10 and 30 m. The winter season D26 lay at greater depth (~100 m) in the central Bay. Along the B-B1 transect during 22-28 April, zonal gradients in temperature and salinity are weak, and MLD varied between 20 and 40 m (Fig. 5e). After one week of the passage of Nargis, the temperature and salinity structures indicate the occurrence of intense vertical mixing (Figs. 5c, 5f and Figs. 6c, 6f). Interestingly, MLD shoaled and D26 deepened in the central Bay during Nargis (Figs. 5e) compared to prior to Nargis (Fig. 5d); moreover, northward shoaling of MLD and deepening D26 is more evident along both the sections (Fig. 5c).

[11] *3.4 Spatio-temporal evolution of SST and SSS along 90°E from RAMA buoys data*

RAMA buoy temperature and salinity data in the upper layer along 90°E at locations 4°N, 8°N, 12°N and 15°N are examined for the spatio-temporal evolution of SST and SSS during January – June, 2008. The 5-day averages of SST and SSS along 90°E (Figs. 7a-b) show strong meridional gradients in temperature from January to March. From the last week of March to the last week of April 2008, prior to Nargis, a northward propagating warm water band is evident (Fig. 7a). However, the meridional salinity gradients persisted from January to May 2008 (Fig. 7b) and the gradients intensified northward in the warm water band (Figs. 7a-b). Persistence of meridional salinity gradients from January to the first week of May is also noticed from the Argo salinity sections (Figs. 6a-b) suggesting the seasonal spread of net freshwater input. This freshwater input is due to the combined effect of advection of river runoff towards central Bay from the northern BoB and the

precipitation minus evaporation over the Bay) from January to the first week of May 2008. Sengupta *et al.* (2006) reported the BoB annual mean precipitation, evaporation and river runoff as 4700 km^3, 3600 km^3 and 2950 km^3 respectively. The part of river runoff into northern BoB is at its minimum in February/March and increases to its maximum in August (Sengupta *et al.*, 2006). These authors also reported a negative net freshwater input of -200 km^{3}month^{-1} in January/February and its increase to 900 km^{3}month^{-1} in August. The occurrence of very low salinity waters in the central Bay during January – April, 2008 is most likely related to the variability of river run off during the previous year and the monsoonal precipitation. The occurrence of low salinity (<32.5 psu) waters over a thick layer (~up to 30 m) in the central Bay during March-April indicates their crucial role in the development of the spring mini-warm pool in the central Bay (Figs. 6 and 7b), which paves the way for the pre-monsoon cyclones like Nargis and the onset of summer monsoon over the BoB. Yu and McPhaden (2011) reported that the surface warming associated with downwelling Rossby Waves is a plausible mechanism for the formation of the observed min-warm pool in the BoB. The surface low salinity waters enhance salinity stratification and the formation of barrier layer, which facilitates surface warming by trapping the net heat flux near the surface (above the barrier layer) during spring months (Pankajakshan *et al.*, 2007).

[12] *3.5 Seasonal evolution of upper ocean temperature, salinity and density structures from RAMA buoy data at 15°N, 90°E*

The time evolution of the daily mean upper ocean temperature, salinity and the computed density profiles measured by RAMA buoy at 15°N, 90°E during January – June 2008 is examined. Figs. 8a-c presents the seasonal evolution of upper ocean structures of temperature, salinity and density from January – June 2008. The MLD, defined as the depth at which density is 0.2 kgm^{-3} higher than the sea surface density, is estimated and its 5-day and 21-day running mean values are also depicted in the density structure (Fig. 8c). During second half of March – April, one can notice a thin (20-30 m) warm layer (T>28°C) coinciding with the very low (<32.5 psu) salinity waters (Figs. 8a-b) and a shallow (<20 m) MLD (Fig. 8c). Thus, Nargis developed over the pre-conditioned warmer, low salinity and shallow MLD region in the central Bay. This is very much supported by the high HC30 and CHP during 26-28 April computed from the high resolution RAMA data (Figs. 4f, 4h) when the first intensification of Nargis took place. Through Nargis's impact on air-sea interaction processes and mixed layer dynamics, the surface waters cooled and MLD deepened in the vicinity of the storm track (Fig. 8c). Nargis moved eastward leaving behind a cool SST wake and it further intensified a

second time on 1 May 2008 over warm SSTs in shallow mixed layer (Fig. 4) on its way towards Myanmar coast.

[13] *3.6 Variations of wind speed and wind stress curl during Nargis*

The satellite measurements of ocean surface vector winds and the derived wind stress curl fields during Nargis period shows the region of strong winds and positive wind stress curl (Figs. 9a-d) beneath the Nargis on 28 April 2008 (Figs. 9a&c) and 2 May 2008 (Figs. 9b &d). This indicates the occurrence of divergence in the upper ocean beneath Nargis and led to intense upwelling at the base of the mixed layer on 28 April and on 2 May. The shoaling (deepening) of the D26 in the central (northern) Bay (Figs. 5c, 5f) signifies the large scale impact of cyclone-induced divergence from greater depths around the cyclone track (downwelling away from the cyclone track on the periphery of divergence). Regions of curl- induced upwelling facilitated surface cooling along and away from the track of the cyclone (Figs. 9c-d).

[14]*3.7 Variations of air-sea heat fluxes and upper ocean heat budget during Nargis*

Table 1 shows the RAMA buoy measured daily averaged net short wave (NSW) and net long wave radiation and fluxes of latent heat (LHF), sensible heat, total heat loss and surface Net Heat Flux (NHF) at 15°N, 90°E during 22-30 April, 2008. Unfortunately, there were no surface meteorological data from RAMA buoy after 30 April. Fig 10a represents the RAMA data derived daily variations of NSW, LHF and NHF during 22-30 April 2008, with each curve fitted to linear trend line (Fig. 10). Under the impact of cyclone Nargis and associated higher cloudiness and stronger winds, the NSW shows a decreasing trend, the LHF shows an increasing trend (LHF is a loss component and shown as negative values) and the NHF exhibits a decreasing trend. The negative NHF and its decreasing trend imply the net heat loss across the sea surface during Nargis. In order to substantiate the observed RAMA buoy data, we have also examined the National Center Environmental Prediction (NCEP) Reanalysis data on NSW, LHF and NHF during 22 April – 4 May 2008. The time variations of NCEP fluxes including the trend lines (Fig. 10b) agree quite well with those from the RAMA buoy (Fig 10a). The NCEP NSW shows minimum value on 1 May, the NCEP LHF shows the higher value on 1 May (large negative value of heat loss), and led to the large decrease in NCEP NHF to a minimum on 1 May. This agreement between the observed and reanalysis data for the Nargis period gives confidence in the overall behavior of the surface fluxes prior to and during the passage of Nargis.

[15] Using the above RAMA data trends, the NSW, LHF and NHF values are extrapolated for 1 May, 2 May and 3 May and the extrapolated values are provided in Table 1 (shown in italics). The NHF decreased from 160.85 Wm^{-2} on 22 April to -103 Wm^{-2} on 1 May amounting to a change of -264 Wm^{-2} across the air-sea interface over 10 days. The daily heat content in the top 30m computed from RAMA buoys also showed a cooling trend (Fig.10c).

[16] Table 2 provides the details of the rate of change of upper layer heat content (Wm^{-2}) over the 10 day duration at various depths where Argo floats available along transects A-A1 and B-B1. Negative (positive) values represent heat loss (gain) in each layer. The large negative values suggest higher heat loss from the upper oceanic layer for the floats closer to the Nargis cyclone track, for example, float #672 along transect A-A1 and floats #673, #755 and #675 along transect B-B1. Float #675 is located to the left of the track and the floats #673 and #755 are located on the right of the track. The float #672 is located on the right of the track, but slightly away from it (Fig. 1c). However, for floats #882, #756, #670 that are further away from the cyclone track, less heat loss or even occasionally heat gain is observed. Interestingly, the floats #673 and #755 that are closer to the cyclone track showed similar upper ocean heat loss in all layers. The heat loss is ~550 Wm^{-2} in the upper 100 m layer and ~290 Wm^{-2} in the sub-layer 75-100 m. This surface heat loss is nearly equivalent to the reduction of oceanic heat content in the 0-30 m layer (Table 2) for #763 and #755 and in the 0-100 m layer for float #762. The heat content reduction in the 75-100 m sub-layer for floats #763 and #755 is as large as ~290 Wm^{-2} and suggests that this reduction in heat content could be associated with the cyclone induced upwelling from depths greater than 100 m. The 75-100 m sub-layer showed heat gain at the floats far away from the cyclone track, and could be associated with the downwelling on the periphery of divergence zone.

[17] The rate of change of temperature over the duration of Nargis can be compared to the average NHF across air-sea interface during the same period by dividing net heat flux by the product of water density (ρ), specific heat capacity of water (Cp) and the thickness (h) of the water column over which heat is distributed. If we take an average NHF of about -50 Wm-2 over the period of Nargis's passage by the buoy at 15°N, 90°E (28 April to May 2), h of 30 m, ρ=1023 Kgm^{-3}, and Cp=4000 JKg^{-1}, the change in water temperature would be about -0.4°C of cooling . The actual rate of cooling is much higher. This result indicates that surface cooling is mainly forced by vertical mixing during Nargis.

Similar observations of SST, SSS and MLD, heat content, heat fluxes for cyclone Laila from six Argo floats (Fig.a-f) are included in this study for comparison and to show some of the factors that

are responsible in restricting Laila to a category 1 cyclone. Along with the high SST, there should be a sufficiently thick layer of warm water which is a necessary precondition for the intensification of a cyclone (*Leipper and Volgenau* 1972; *gray* 1979; *Holliday and Thompson* 1979; *Emanuel* 1999; *Shay et al.,* 2000; *Coine and Uhlhorn* 2003; *Emanuel et al.,*2004; *Lin et al.,* 2005; Part I). Cyclone Laila moved in a northwest direction towards the western Bay (Fig.11a) which is weakly stratified (Fig.12c) with MLD's of about 100m. Hence the above condition is not satisfied in this case. There is a drop in CHP of 36Wm^{-2} (Fig. 11e) and a heat loss in the top 30m of about 22 Wm^{-2} (Fig.11f). Net heat flux (NCEP/NCAR) from 14-24 May 2010 is about 28 Wm^{-2}, which is equal to the heat content change in the upper 50m (for Agro floats #882 and #883) and 100m (for floats #107 and #783). Along section CC1, a weak stratification with heat loss decreasing towards C1 is observed (Fig.12d); this may be in response to cooling caused by upwelling at the center of the cyclone. This cooling results in the supply of air-sea flux from the ocean that is essential for storm intensification (*Price* 1981; *Gallacheret.al.,* 1989;,*Emanuel* 1999, and *Emanuelet al.,*2004 *Cione and Uhlhorn* 2003; *Lin et.al.,* 2005,2009 Part I; *Wu et al.,* 2007) and cut off the supply of heat and resulting in the decay of cyclone. This is may be the root cause in case of cyclone Laila to end up as a category 1. Hence the analysis of 3-D structure of upper ocean along with meteorological parameters is crucial in understanding the intensification/decay of tropical cyclones.

Conclusions

[19] We have demonstrated the utility and the importance of observational data from RAMA buoys and Argo floats to describe and understand the oceanic processes associated with extreme weather events like cyclone Nargis and Laila over the BoB. These *in-situ* observations in the upper ocean together with the satellite measurements provided a 3-D description of the structure of upper ocean variability associated with ocean-atmosphere interactions due to cyclone Nargis. The observations further indicate that the pre-conditioning of the central BoB with warmer and less saline waters contributed to the intensification of Nargis where as the weak stratified high saline water in the western bay hindered the intensification of the cyclone Laila. In response to Nargis, a vast surface area of BoB cooled with a maximum drop in SST about 2°C due to air-sea heat fluxes and ocean mixing associated with the storm, which is in agreement with the earlier studies (Subrahamanyam *et al.,*2005, Sengupta *et al.*, 2007). Further, an increase in the sea surface salinity, deepening of the mixed layer, shoaling of D26 and loss in upper ocean heat content also occurred during Nargis. Under the influence of Nargis, the net shortwave radiation, though large and positive, showed a decreasing trend while the latent heat flux showed an increasing trend contributing to the decrease in

the net surface heat flux over the observational period. The upper ocean heat content computed at various depths using Argo data revealed that maximum heat loss is from 0 – 100 m depth in association with cyclone-induced divergence from deeper depths.

Acknowledgments

References

Anonymous, 1979. Tracks of Storms and Depressions in the Bay of Bengal and the Arabian Sea 1877–1970. India Meteorological Department, New Delhi, Charts :1–186.

Behra, S.K., Deo,A.A., and Salvekar,P.S., 1998. Investigation of Mixed layer response to Bay of Bengal cyclone using a simple ocean model.Meteorol. Atmos. Phys., 65, 77-91.

Chintalu, G.R., Seetaramayya, P.,Ravichadran,M., and Mahajan,P.N.,2001. Response of the Bay of Bengal to Gopalpur and Paradip super cyclones during 15-31 October 1999.Curr. Sci., 81, 3, 283-291.

Coine, J.J., and Uhlhorn,E.W.,2003. Sea surface temperature variability in hurricanes: Implications with respect to intensity change.Mon.Wea.Rev.,131, 1783-1796.

Emanuel, K.A., 1999. Thermodynamic control of hurricane intensity.Nature 401,665-669

Emanuel, K.A., DesAutels, C.,Holloway C., and Korty,R.,2004. Environmental control of tropical cyclone intensity. J.Atmos.Sci., 61, 843-858.

Gallacher,P.C., Rotunno,R., and Emanuel, K.A.,1989. Tropical cyclogenesis in the coupled ocean-atmospheric model. Preprints 18th Conference on Hurricanes and tropical meteorology. SanDiegeo,CA , Amer.Meteor.Soc., 121-122.

Gray,W.M., 1997. Tropical cyclone genesis in the western North Pacific.J.Meteor.Soc. Japan, 55, 465-482.

Holliday,C.R., and Thompson,A.H.,1979. climatological characteristics of rapidly intensifying typhoons. Mon.Wea.Rev., 107, 1022-1034.

Gopalakrishna, V.V., Murty, V.S.N.,Sarma M.S.S. and Sastry J.S.,1993. Thermal response of upper layers of Bay of Bengal to forcing of a severe cyclonic storm: A case study.Indian J. Mar. Sci., 22, 8-11.

Leipper, D., and Volgenau,D.,1972. Hurricane heat potential of Gulf of Mexico.J.Phys. Oceanogr., 2, 218-224

Lin, I.I., Wu, C.C.,Emanuel, K.A.,Lee, I.H., Wu, C.R., and Pune,I.F.,2005. The interaction of Super typhoon Maemi (2003) with warm core eddy.Mon.Wea.Rev.,133, 2635-2649.

Lin, I.I., Chen , C.H.,Pun, I.F., Liu ,W.T.,and Wu,C.C.,2009. Warm ocean anomaly , air sea fluxes, and the rapid intensification of tropical cyclone Nargis (2008).Geophysical.Res.Lett., 36, L03817, doi:10.1029/2008GL035815

Pankajakshan, T., Muraleedharan, P.M.,Rao, R. R.,Somayajulu, Y.K.,Reddy,G.V.,and Revichandran, C.,2007. Observed seasonal variability of barrier layer in the Bay of Bengal. J. Geophys. Res., 112, C02009, doi:10.1029/2006J003651.

Price, J.F.,1981. Upper Ocean response to a Hurricane, *J. Phys. Oceanogr., 11*, 153–175.

McPhaden, M.J., Foltz, G.R., Lee, T.,Murty, V.S.N.,Ravichandran, M., Gabriel Vecchi, Jerome Vialard, Wiggert,J.D.,and Lisan, Yu (2009a), Ocean-Atmosphere Interactions during cyclone Nargis, *Eos Trans. Am. Geophys. Union*, *90*(7), 53-54.

McPhaden, M.J., G. Meyers, K. Ando , Y. Masumoto, V.S.N. Murty**,** M.Ravichandran, F. Syamsudin, J. Vialard, L. Yu and W. Yu (2009b), RAMA: The Research Moored Array for African–Asian–Australian Monsoon Analysis and prediction, *Bull. Am. Meteorol. Soc.*, *90*(4), 459-480.

Meyers, G. and R. Boscolo (2006), The Indian Ocean Observing System (IndOOS). *CLIVAR Exchanges*, *11*(4), International CLIVAR Project Office, Southampton, UK, p. 2-3.

Murty, V.S.N., Y.V.B. Sarma and D.P. Rao (1996), Variability of the oceanic Boundary layer characteristics in the northern Bay of Bengal during MONTBLEX-90, *Proc. Indian Acad. Sci. (Earth Planet Sci.)*, *105*, 41-61.

Muthuchami, A. and Dhanavanthan, P. (2007), Probable storm motion in the Bay of Bengal in April and May. *J. Ind. Geophysical Union*, *11*(4), 209-215.

Novlan, D.J. and Gray W.M (1974), Hurricane spawned tornadoes, *Mon. Wea. Rev*., *102*, 476-488.

Obasi, G.O.P. (1997), WMO's Programme on Tropical Cyclone, *Mausam*, *48*,103–112.

Rao, R.R. (1987), Further analysis on the thermal response of the upper Bay of Bengalto the forcing of pre-monsoon cyclonic storm and summer monsoon onset during MONEX-79, *Mausam,38*, 147-156.

Sadhuram, Y., B.P. Rao, D.P. Rao, P.N.M. Shastry and M.V. Subrahmanyam (2004), Seasonal variation of cyclone heat potential in the Bay of Bengal, *Natural Hazards*, *32*, 191-209.

Sadhuram, Y. (2004), Record decrease of sea surface temperature following the passage of a super cyclone over the Bay of Bengal, *Current Sci.*, *86*, 3, 383-384.

Saji, P.K., S.S.C. Shenoi, A. M. Almeida and L.V.G. Rao (2000), Inertial currents in the Indian Ocean derived from satellite tracked surface drifters. *Oceanologica Acta*, *23*(5), 635-640.

Sarma, Y.V.B., V.S.N. Murty and D.P. Rao (1990), Distribution of cyclone heat Potential in the Bay of Bengal, *Ind. J. Mar. Sci.*, *19*, 102-106.

Sengupta, D., G.N. Bharathraj and S.S.C. Shenoi (2006), Surface freshwater from Bay of Bengal runoff and Indonesian throughflow in the tropical Indian Ocean, *Geophysical Res. Letts., 33*, L22609, Doi:10.1029/2006GL027573.

Sengupta, D., G.N. Bharathiraj and D.S. Anitha (2007), Cyclone-induced mixing does not cool SST in the post-monsoon north Bay of Bengal, *Atmos. Sci. Let*. Doi:10.1002/asl.162.

Shay, L.K., G.J.Goni and P.G. Black (2000), Effects of warm oceanic features on hurricane opal, *Mon.Wea.Rev., 128,* 1366-1383

Subrahmanyam, B., V.S.N. Murty, Ryan J. Sharp and James J.O'Brien (2005), Air-sea coupling during the tropical cyclones in the Indian Ocean: A case study using satellite observations, *Pure Appl. Geophys.*, *162*, 1643-1672. Doi: 10.1007/s00024-005-2687-6.

Vinayachandran, P.N., V.S.N. Murty and V. Ramesh Babu (2002), Observations of barrier layer formation in the Bay of Bengal during summer monsoon, *J. Geophys. Res.*, *107*, C12, SRF 19-1 to SRF 19-9, doi:10.1029/2001JC000831.

Wu.C.C., C.Y. Lee and I.I. Lin (2007), the effect of ocean eddy on tropical cyclone intensity, *J.Atmos.Sci.,64*, 3562-3578.

Yu, Lisan, Michael J. McPhaden (2011), Oceanic Preconditioning of cyclone Nargis in the Bay of Bengal: Interaction between Rossby Waves, Surface freshwaters, and Sea Surface Temperatures, *J. Phys. Oceanogr.*, **41**, 1741-1755, doi:10.1175/2011JPO4437.1

Legend to the Figures

Fig 1. Cyclone tracks in the Bay of Bengal in May during (a) 1945-1970 and (b) 1971
-2008. The cyclone tracks of Nargis (Red line) & Laila (Blue line) are shown in (b). (c)
Laila track and Argo float locations with the depiction of C-C1 transect (d) Nargis track and
Argo float locations with the depiction of A-A1 and B-B1 transects. The black rectangles
indicate the regions over which Laila and Nargis cyclones intensified.

Fig 2. Estimated change in (a) Sea Surface Temperature (SST, °C) anomaly, (b) Sea Surface
Salinity (psu), (c) Depth of 26°C isotherm (D26, m), (d) Mixed Layer Depth (MLD, m), (e)
Cyclone Heat Potential (CHP, Wm^{-2}) and (f) Heat Content in 0-30 m layer (HC30,Wm^{-2})
after and before Nargis over the 10-day interval of Argo data. Nargis's track is shown in the
black thick line. Rectangles (black color) indicate the regions over which Nargis
intensified, small rectangular symbols indicating the Argo floats.

Fig 3. RAMA buoy measured (a) daily averaged zonal and meridional currents at
10 m depth from 1 April – 31 May 2008 and (b) 2-hourly current vectors
during 29 April – 5 May 2008. Large amplitude inertial cycles are observed during 30 April
– 2 May in (a) and (b). Each inertial cycle has a period of about 2 days (48 hours)
corresponding to the local (latitude) inertial frequency of 46.4 hours.

Fig 4. Daily and 10 day averages of RAMA buoy measured and the estimated
parameters and the corresponding 10 day interval Argo data (#755) during March – May
2008 for (a) SST, (b) SSS, (c) wind speed, (d) net surface heat flux, (e) MLD, (f) heat
content to 30 m depth, (g) depth of 26°C isotherm and (h) cyclone heat potential. The 10
day averages of RAMA buoy data are included for comparison with 10 day interval Argo
data.

Fig 5. Vertical sections of Argo temperature in the upper 100 m along the
A-A1transect (left panel) and B-B1transect (right panel) during (a & d) first week of January, (b & e)
one week before (22-28 April) Nargis and (c & f) after (1-4 May) Nargis. The data points
(vertical dotted line) and variation of MLD (horizontal dashed line) are also shown.

Fig 6. Vertical sections of Argo salinity in the upper 100 m along theA-A1 transect (left panel) and
B-B1transect (right panel) during (a & d) first week of January, (b & e) one week before
(22-28 April) Nargis and (c & f) after (1-4 May) Nargis. The data points (vertical dotted
line) and variation of MLD (horizontal dashed line) are also shown.

Fig 7. Spatio-temporal evolution of (a) SST and (b) SSS along 90°E in the BoB as measured from
RAMA moorings at Equator, 4°N, 8°N, 12°N and 15°N. Meridional gradients in
temperature and salinity are the noteworthy features. The period of intense spring warming

north of 8°N during March-April co-occurs with the period of lower surface salinities (intense freshening).

Fig 8. Depth-time sections of the RAMA buoy measured upper layer (0-100 m) temperature (upper panel), salinity (middle panel) and density (lower panel) at 12°N, 90°E. The red and green lines in the lower panel denote the 5-day and 21-day running mean mixed layer depth defined by the density criterion (depth at which density is 0.2 kgm^{-3} higher than that of sea surface).

Fig 9. Satellite derived surface wind speed (ms^{-1}, top panel) and the estimated wind stress curl (x10^{-7} Pm^{-1}, bottom panel) on (a & c) 28 April and (b & d) for 2 May during Nargis period. Zones of strong winds and intense divergence (positive wind stress curl) are located beneath the cyclone in the western Bay on 28 April and in the eastern Bay on 2 May. Respective color code scale bars are provided on the right side of the Figures.

Fig 10.Daily variations of (a) RAMA buoy measured and (b) NCEP reanalysis field of shortwave solar radiation and the computed latent heat flux and net heat flux and (c) heat content in the top 30 m computed using RAMA buoys

during Nargis period (22 April – 3 May 2008). The RAMA data were downloaded from (PMEL 2010) and the NCEP daily data were downloaded from (ESRL 2010). Least square fitted linear trend line for each parameter for both data sets is also depicted. Details are given in the text.

Fig 11. Estimated anomalies in (b) Sea Surface Temperature (SST, °C), (c) Sea Surface Salinity (psu), (d) Depth of 26°C isotherm (D26, m), (e) Mixed Layer Depth (MLD, m), (f) rate of change in Cyclone Heat Potential (CHP, Wm^{-2}) and (g) rate of change in Heat Content in 0-30 m layer (HC30,Wm^{-2}) after and before Laila over the 10-day interval of Argo data and the rectangle (black color) indicate the regions over which Laila intensified, small rectangular symbols indicating the Argo floats.

Fig 12. Vertical sections of Argo (a &b)Temperature, (c & d)Salinity in the upper 100m a week before and after Laila cyclone along the C-C1 transect. The data points (vertical dotted line) and variation of MLD (horizontal dashed line) are also shown.

Table headings

Table 1. Daily averaged surface heat at the sea surface during the Nargis period from the RAMA buoy at 15°N, 90°E. [Source: http://www.pmel.noaa.gov].   As RAMA data were not available, the predicted net shortwave radiation, latent heat flux and net heat flux using the linear trend lines from 1st to 3rd May 2008 are shown in italics. Units are in Wm^{-2}.

Table 2. Estimates of change of upper layer heat content (after and before Nargis) over 10 day period during Nargis in different layers.   The estimations are based on the computed upper layer heat content using Argo temperature profiles. Negative values indicate upper layer heat loss, positive values indicate heat gain. Estimates for the Argo floats on the right of Nargis track are marked in bold and italics. Units are given in Wm^{-2}.
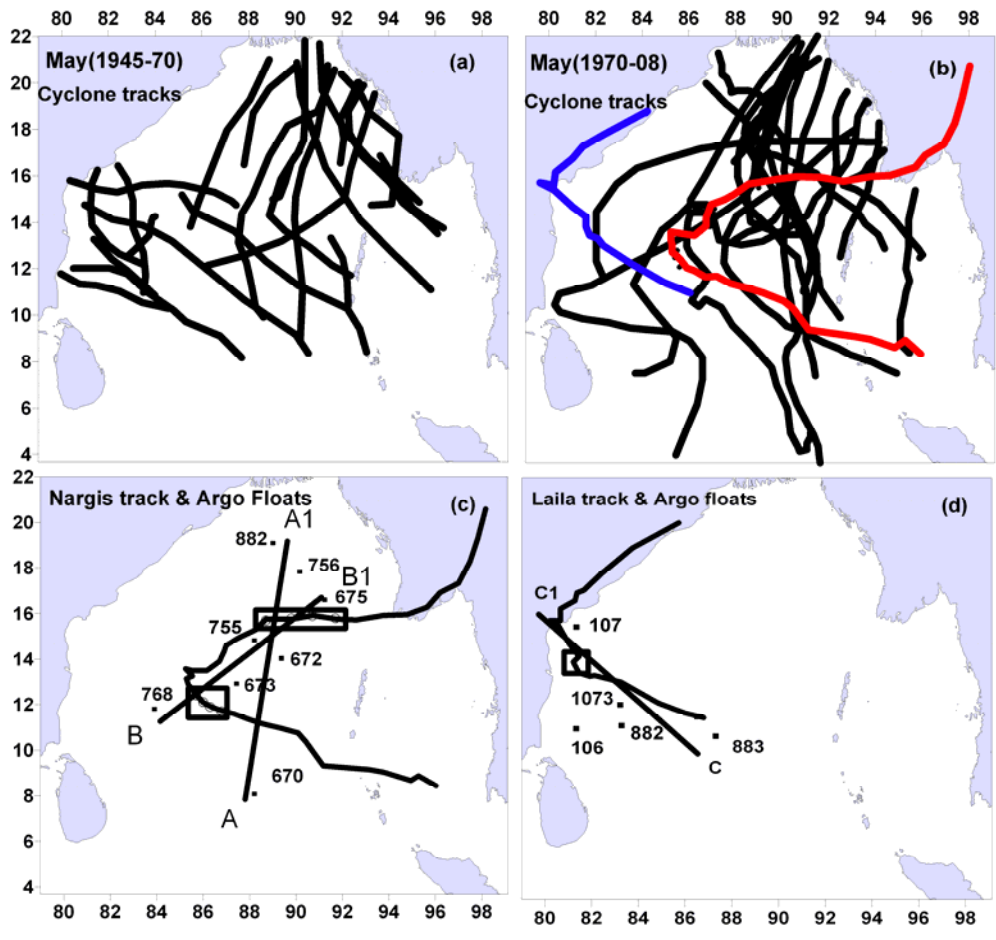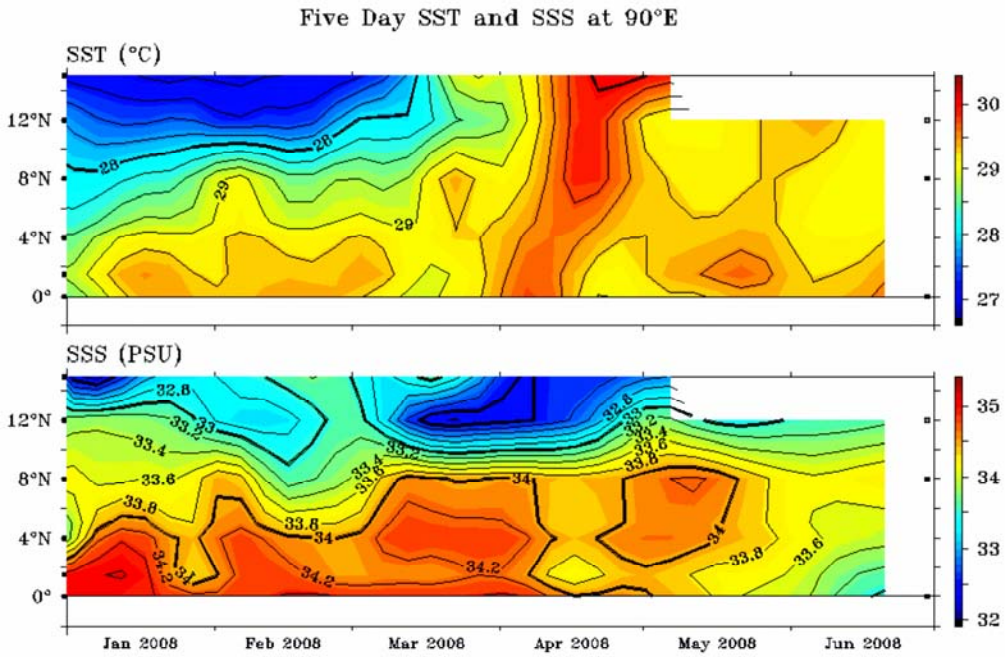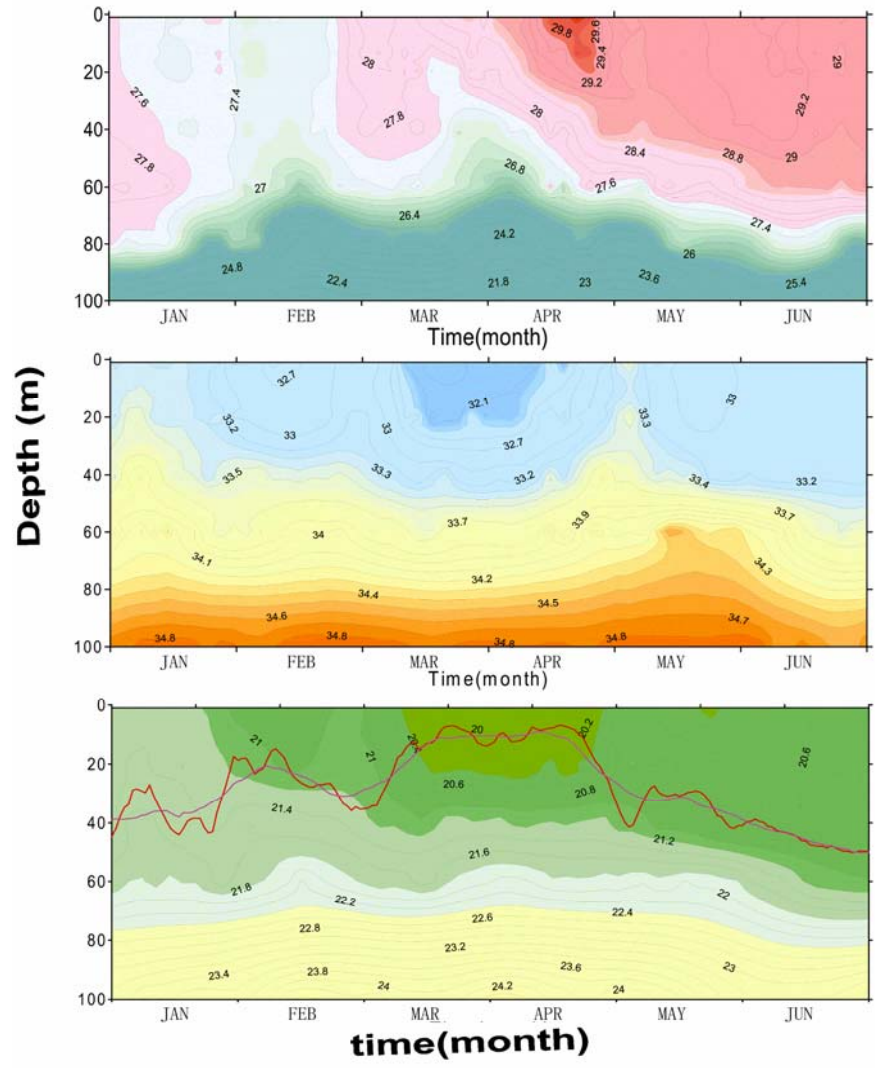
Fig 1.
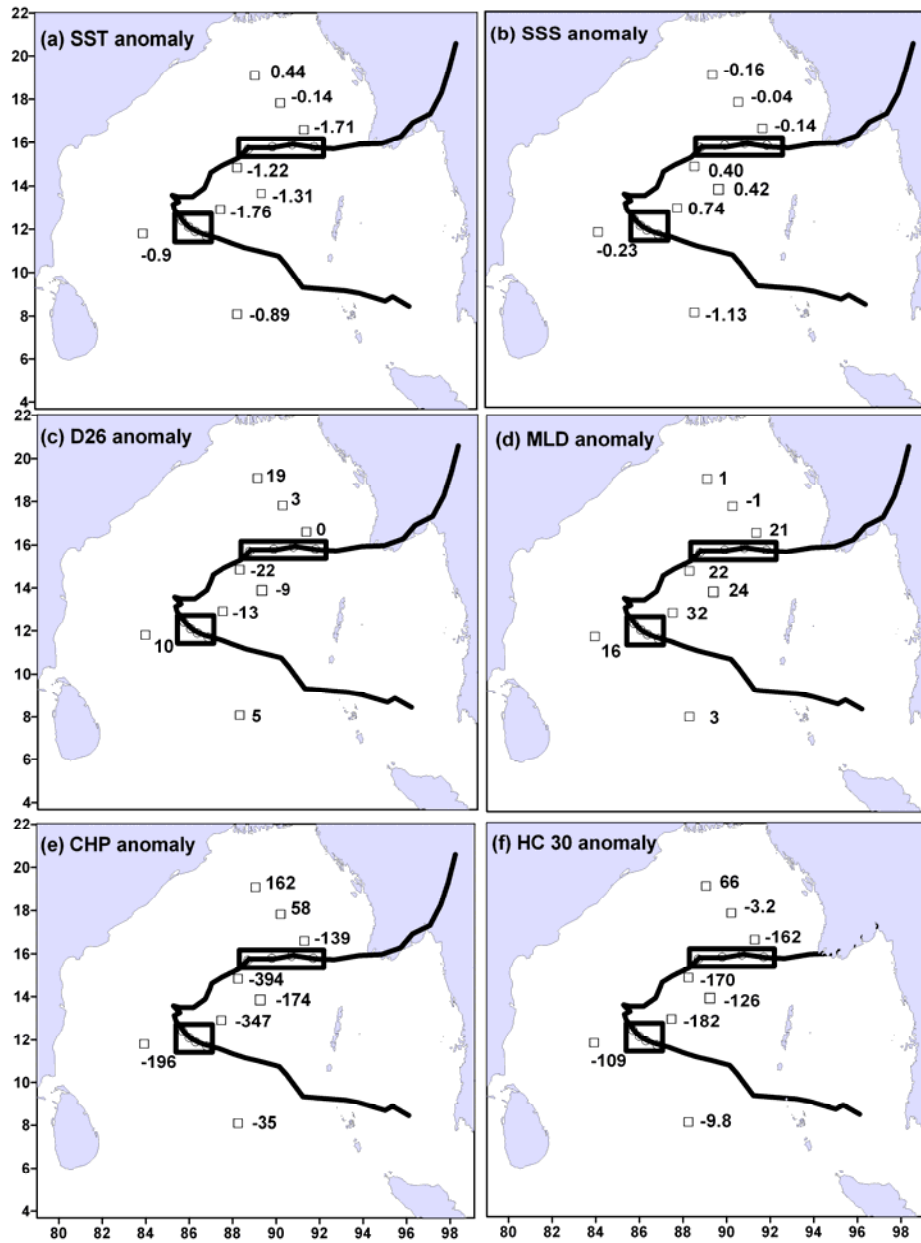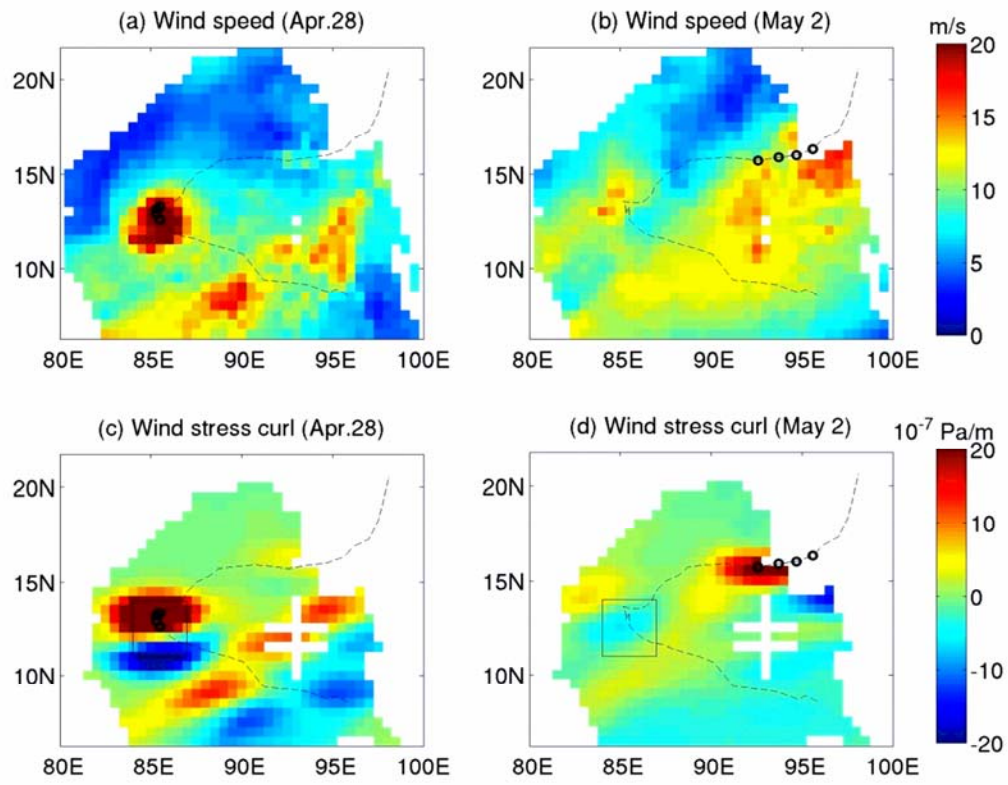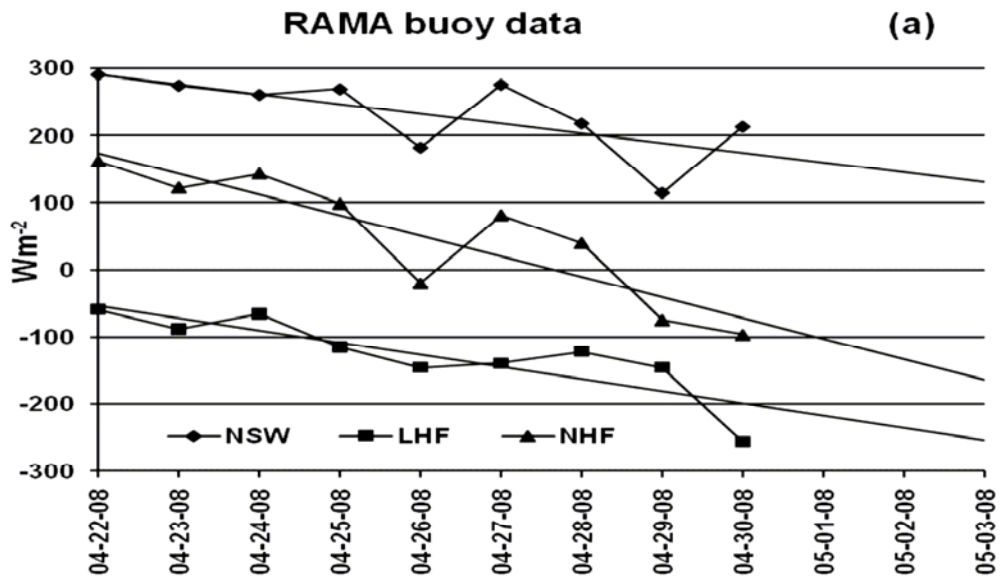
Fig 2.
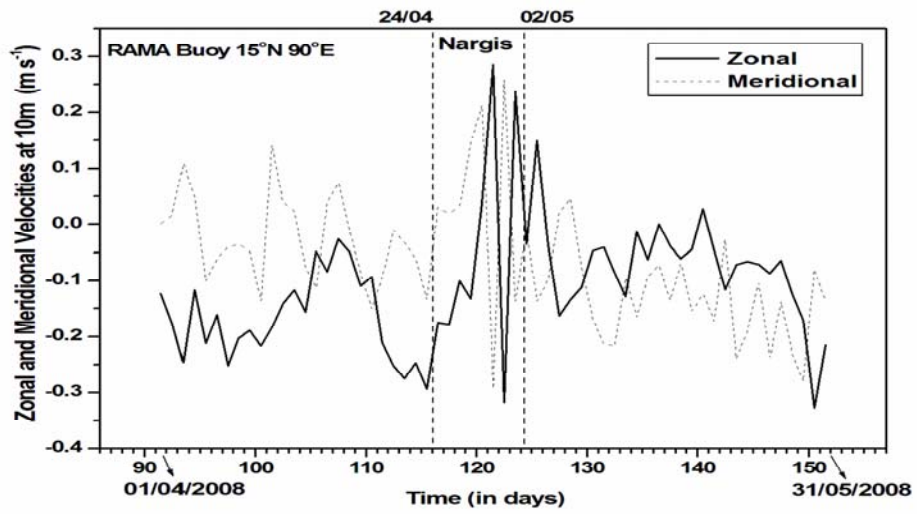
Fig 3a.
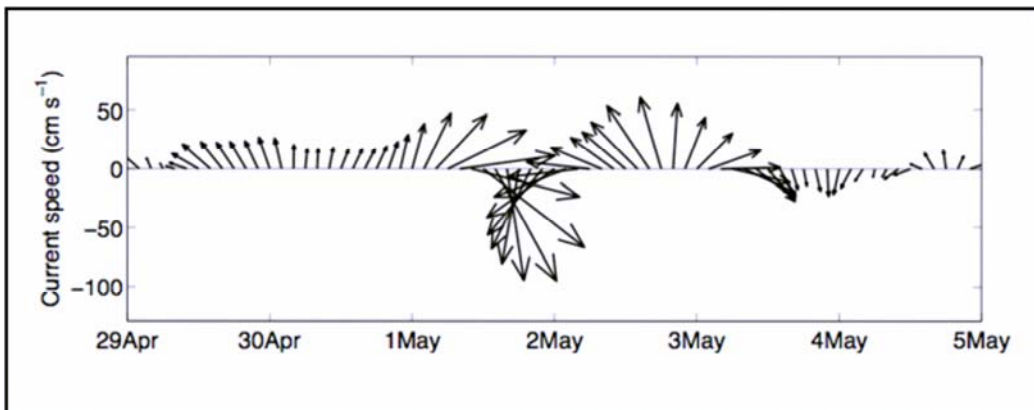
Fig 3b.
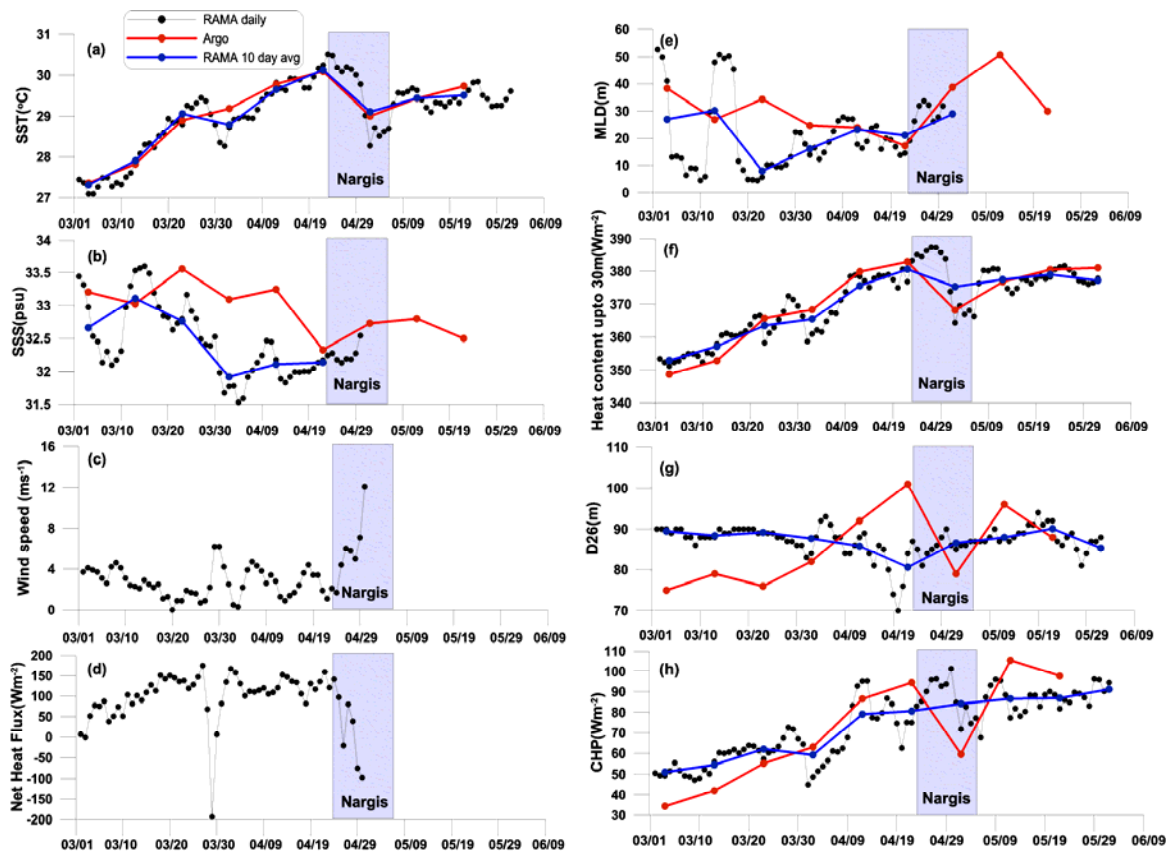
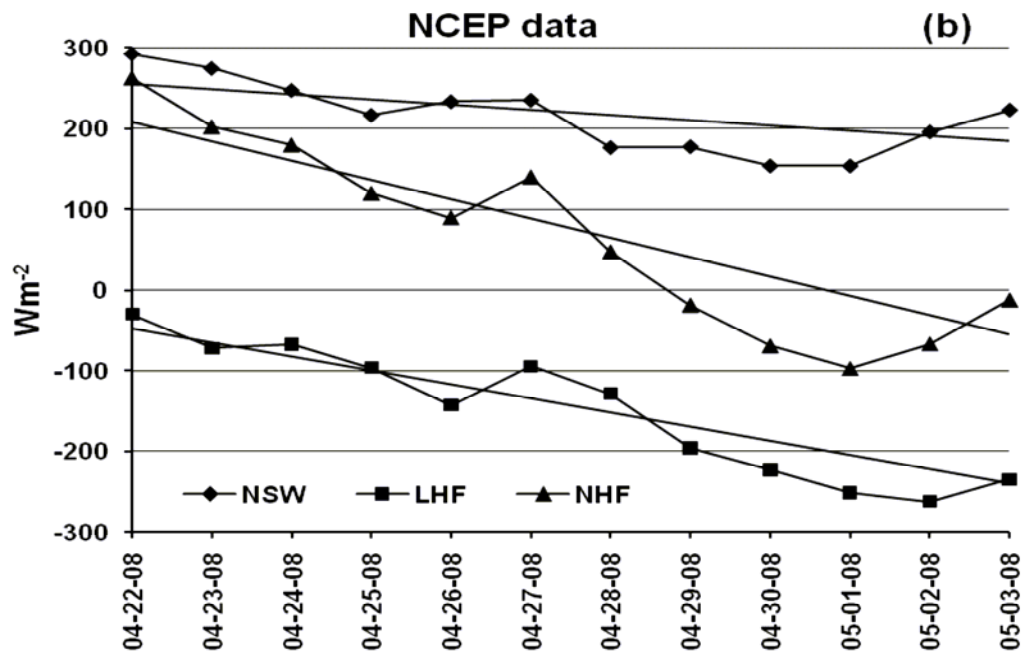Fig 4.
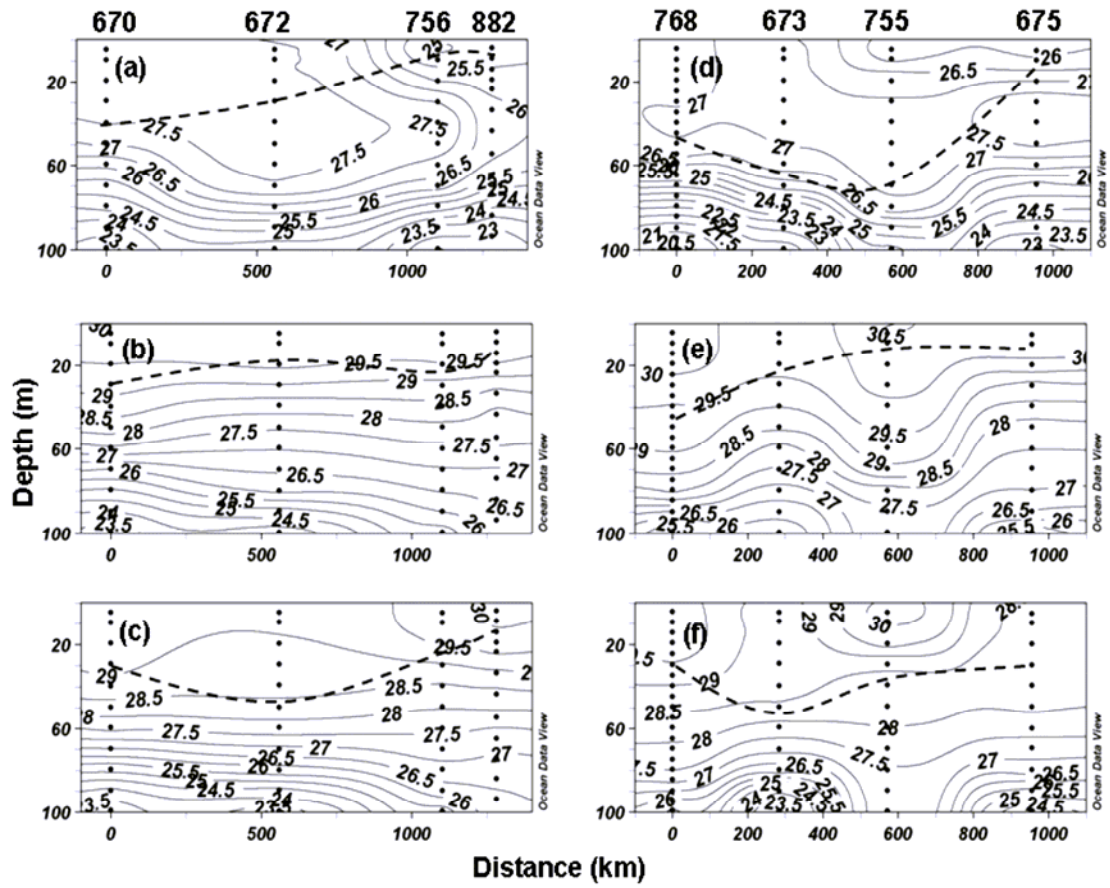
Fig 5.
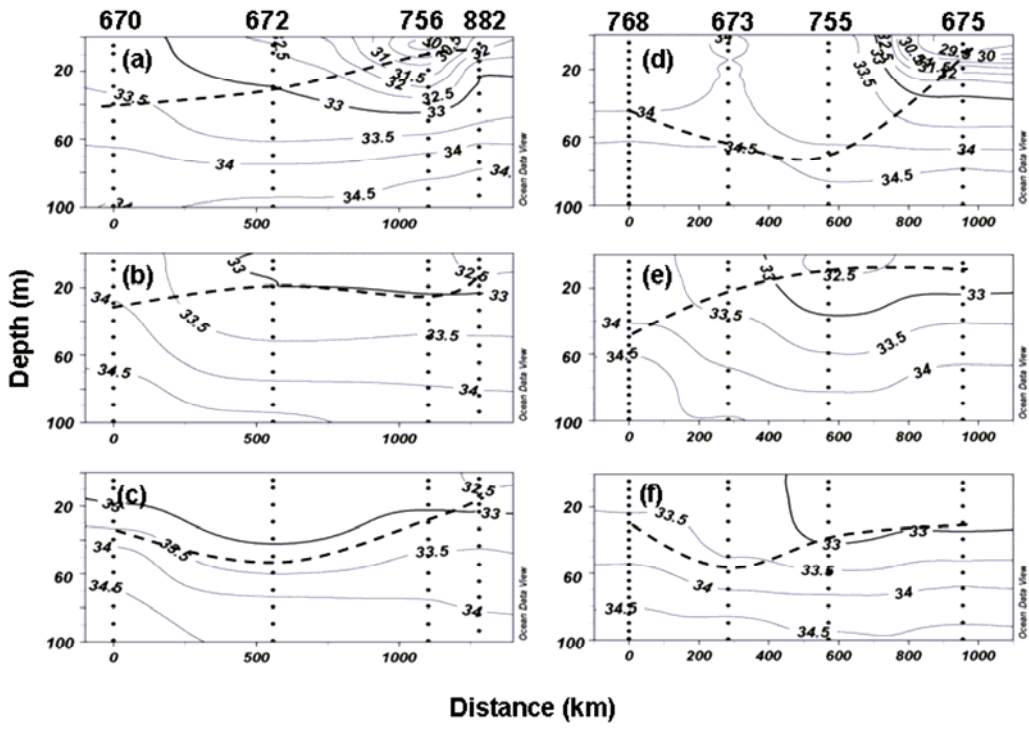
Fig 6.

Fig 7.
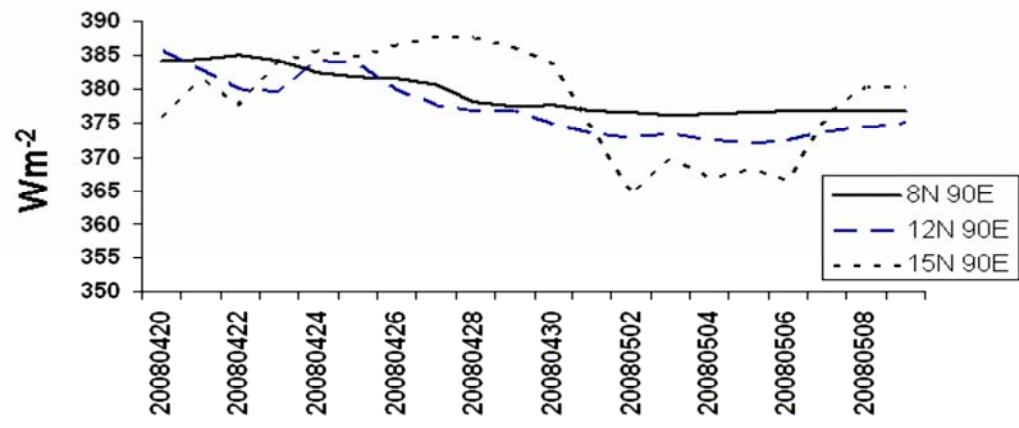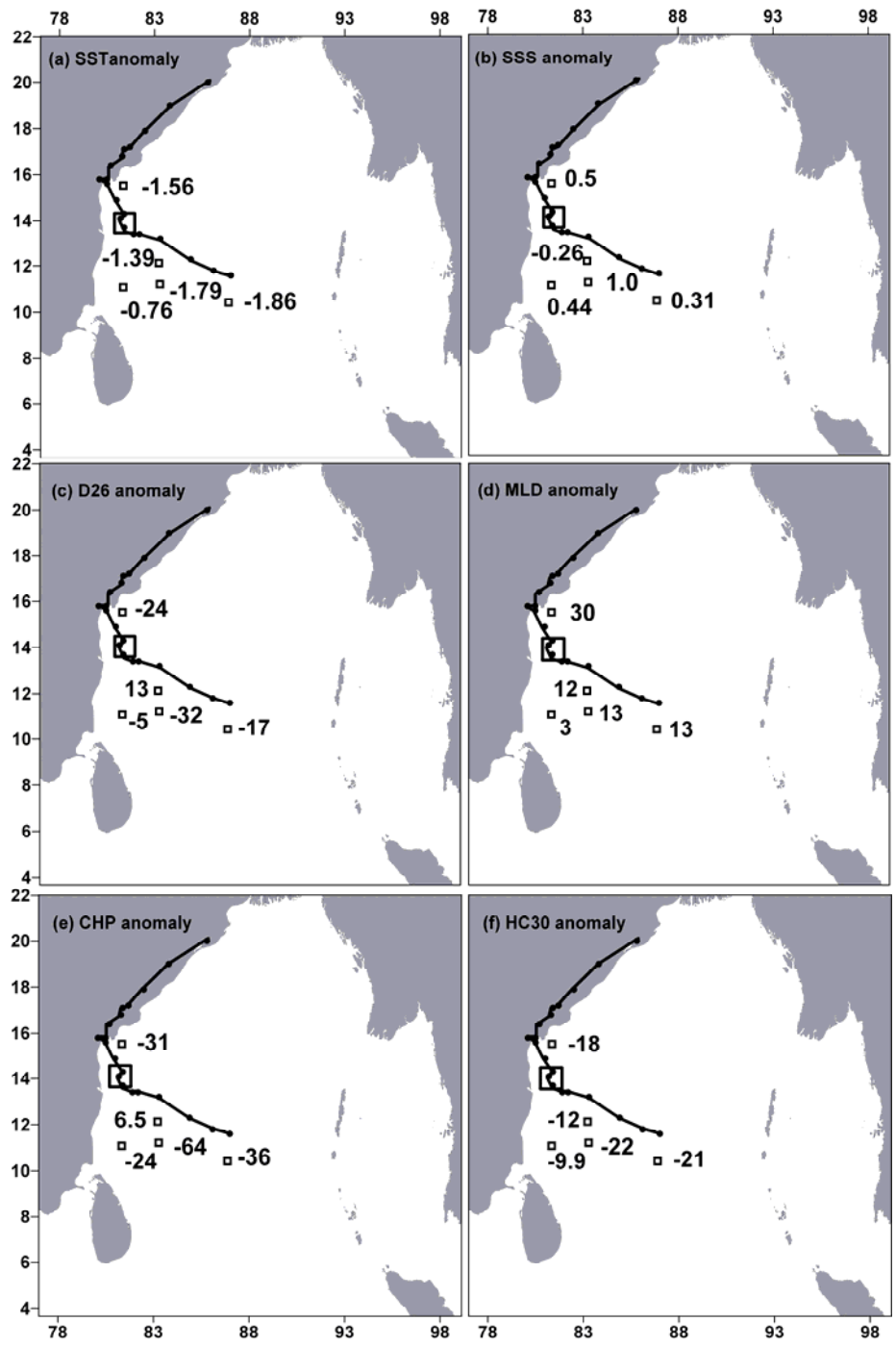
Fig 8.

Fig 9.

Fig 10 a.

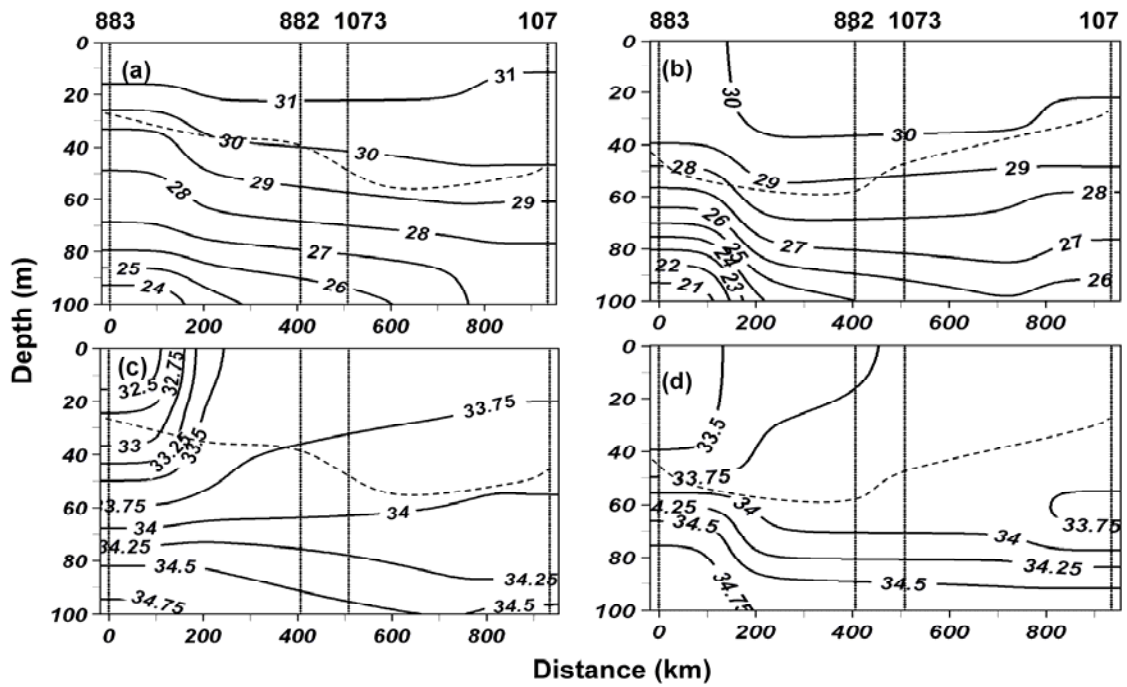Fig 10 b.

Fig 10c.

Fig 11.

Fig 12.

Table 1

Date	Net Short wave radiation	Net Long wave radiation	Latent Heat flux	Sensible Heat flux	Total heat loss	Net heat flux
04/22/08	291.06	-68.24	-59.48	-2.49	-130.21	160.85
04/23/08	274.82	-59.64	-88.31	-4.78	-152.73	122.09
04/24/08	261.23	-48.74	-66.02	-3.71	-118.47	142.76
04/25/08	269.56	-49.94	-115.39	-5.67	-171.00	98.56
04/26/08	181.80	-45.36	-145.85	-10.98	-202.19	-20.39
04/27/08	276.15	-45.38	-139.55	-9.74	-194.67	81.48
04/28/08	217.78	-43.95	-121.88	-12.17	-178.00	39.78
04/29/08	113.78	-34.54	-145.72	-8.17	-188.43	-74.65
04/30/08	212.96	-35.07	-255.74	-18.35	-309.16	-96.20
05/01/08	*160.30*	---	*-217.34*	---	---	*-103.00*
05/02/08	*145.71*	---	*-235.65*	---	---	*-133.69*
05/03/08	*131.12*	---	*-253.86*	---	---	*-164.38*

Table 2

Argo Float No.	Rate of change in the upper layer heat content in different layers				
	0-30m	0-50 m	0-75 m	0-100 m	75-100 m
Argo floats along A-A1 section (Figure 1c)					
882	66	122	104	353	+149
756	-3	-9	24	64	+40
672	*-126*	*-113*	*-128*	*-307*	*-179*
670	-10	-61	-15	-18	-3
Argo floats along B-B1 section (Figure 1c)					
675	-162	-168	-142	-170	-28
755	*-170*	*-193*	*-277*	*-567*	*-290*
673	*-182*	*-183*	*-255*	*-550*	*-295*
768	-109	-122	-158	-80	+78